

Exciton Scattering in Heterostructures with (In,Ga)As/GaAs Quantum Wells¹

A. V. Trifonov, Yu. P. Efimov, S. A. Eliseev, V. A. Lovtcius, P. Yu. Shapochkin, and I. V. Ignatiev*

Spin Optics Laboratory, St. Petersburg State University, St. Petersburg, 198504 Russia

**e-mail: i.ignatiev@spbu.ru*

Abstract—Reflectance spectroscopy is used to study exciton scattering caused by phonons, nonradiative excitons, and free carriers in a heterostructure with a wide (In,Ga)As/GaAs quantum well. Nonradiative excitons and free carriers are created via additional monochromatic illumination by a tunable laser. Constants of exciton–acoustic phonon and exciton–LO phonon scattering are determined from the temperature variations in the nonradiative broadening of exciton resonances. The excitation spectra of nonradiative broadening reveal sharp resonances associated with exciton–exciton scattering and a smooth background caused by exciton–free carrier scattering.

DOI: 10.3103/S1062873817120292

INTRODUCTION

The behavior of excitons in semiconductor heterostructures can be governed by both fundamental processes and processes caused by different defects in the structures. Progress in the technology of molecular beam epitaxy allows one to grow heterostructures with quantum wells (QWs) of high structural quality [1, 2]. Fundamental processes dominate in such structures, allowing one to study them in detail.

In this work, we consider the scattering of optically active excitons by such quasiparticles as phonons, nonradiative excitons, and free carriers. These processes are studied experimentally for a heterostructure containing a (In,Ga)As QW of width $L = 95$ nm and an indium content of around 2%. The sample's structure and its optical characteristics were described in [3]. The great width of the QW allows us to observe several quantum-confined exciton states in the reflectance spectra and to quantitatively study the broadening of exciton resonances caused by different scattering processes.

EXPERIMENTAL

Reflectance spectra in the spectral range of exciton transitions to quantum-confined states were studied. A femtosecond laser was used as a source of a continuous spectrum. Its radiation was directed approximately along the normal to the sample surface. The sample was placed in a closed-cycle cryostat that allowed the sample temperature to be varied in the wide range of 4–300 K. Relatively low excitation

power (units of microwatts in a spot of about 50 μm in diameter) was used to avoid any notable broadening of the exciton resonances. The maximum of the excitation spectrum was tuned below the lowest exciton transition to avoid the photocreation of excitons, free electrons, and holes in noticeable concentrations. The radiation of a continuous-wave titanium–sapphire laser was used for the controlled creation of excitons and free carriers. Its wavelength was varied over a wide spectral range.

An example of a reflectance spectrum of the investigated heterostructure is shown in Fig. 1. Four exciton resonances, marked as X1, X2, X3, and X4, are observed in the spectrum. The resonant reflectance can be modeled using the phenomenological theory described in [4] for a single exciton transition and generalized for several transitions in [2]. Microscopic modeling shows that this theory can be applied to QWs up to 150 nm wide [5].

In phenomenological theory, the reflectance spectrum is described by the expressions

$$R(\omega) = \left| \frac{r_s + r_{\text{QW}} e^{2i\psi}}{1 + r_s r_{\text{QW}} e^{2i\psi}} \right|, \quad (1)$$

$$r_{\text{QW}} = \sum_{N=1}^{N_{\text{max}}} \frac{i(-1)^{(N-1)} \Gamma_{0N} e^{i\phi_N}}{(\omega_{0N} - \omega) - i(\Gamma_{0N} + \Gamma_N)}. \quad (2)$$

Here, r_s describes the amplitude of reflections from a sample's surface, r_{QW} is the resonant reflection from the QW, and ψ is the phase shift of the light wave during its propagation from the sample's surface to the QW layer. Frequencies ω_{0N} describe the spectral positions of the exciton resonances, and phases ϕ_N are

¹ This article was translated by the authors.

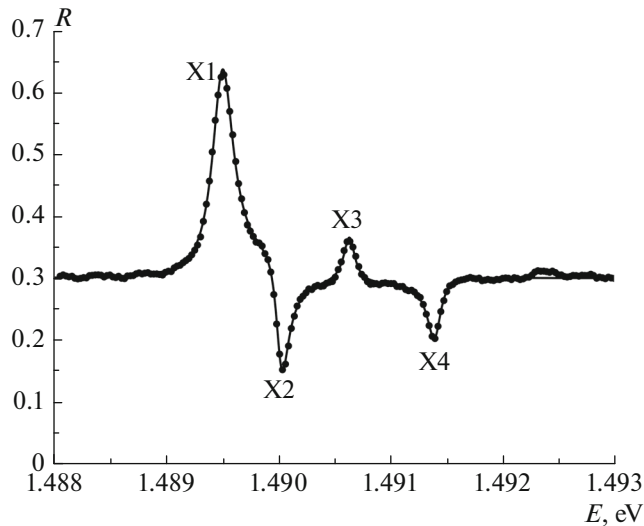


Fig. 1. Reflectance spectrum of the heterostructure with the wide (In,Ga)As/GaAs quantum well in the range of exciton transitions to quantum-confined states X1, ..., X4, measured without additional optical excitation. Points represent experimental data; the solid curve is the fit using expressions (1) and (2).

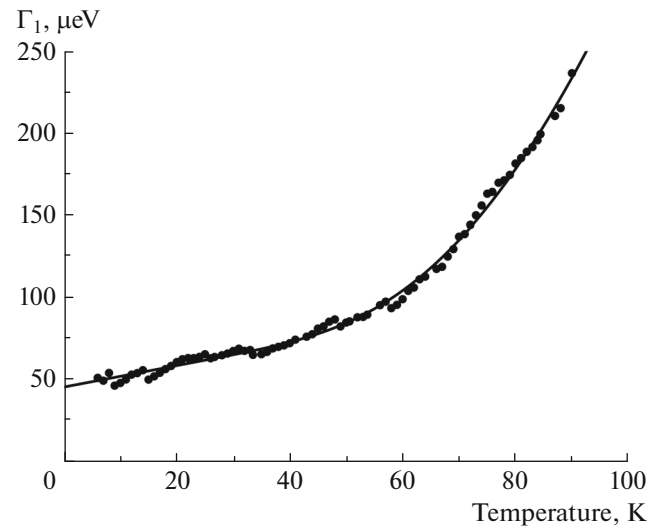


Fig. 2. Temperature dependence of the nonradiative broadening of exciton resonance X1. Points represent the values of Γ_1 (in energy units) obtained from fitting the reflectance spectra with expressions (1) and (2); the solid line is the fit using expression (3).

additional phase shifts in the QW that can vary for different exciton resonances when there is asymmetry in the QW potential [3]. Quantities Γ_{0N} and Γ_N describe the radiative and nonradiative broadenings of the resonances, respectively. Strictly speaking, the model can be applied only to homogeneously broadened resonances. With considerable inhomogeneous broadening (i.e., a statistical spread of the exciton transition frequencies), the reflectance coefficient is determined via the convolution of expression (2) with the contour of inhomogeneous broadening. For high-quality structures with small inhomogeneous broadening, expression (2) can be used in a good approximation if we consider nonradiative broadening to be the sum of homogeneous and inhomogeneous broadenings of the exciton resonances. Below, we focus on the behavior of nonradiative broadening Γ_N characterizing the processes of exciton scattering.

Figure 1 shows the fit of the reflectance spectrum using expressions (1) and (2). We can see that the modeled spectrum describes all important features of the resonances. This allows us to obtain reliable data on the broadening of the exciton resonances and thus to study the processes of scattering quantitatively.

EXCITON-PHONON SCATTERING

The scattering of excitons by phonons in GaAs-based heterostructures at low temperatures is characterized by a relatively small cross section, compared to those of similar processes in other types of semiconductors. The relaxation processes of hot electrons with the emission of acoustic phonons are characterized in

particular by relaxation times on the order of several tens of picoseconds [6] that correspond to the nonradiative broadening of exciton resonances on the order of units of μeV . This broadening is small compared to the radiative broadening of exciton resonances. For example, $\Gamma_{01} \approx 50 \mu\text{eV}$ in the investigated structure.

Exciton-phonon scattering can be enhanced considerably by heating a sample resulting in an increase of the population of the phonon states. Figure 2 presents the results from measuring and processing reflectance spectra at different sample temperatures. It shows the temperature dependence of the nonradiative broadening of the lowest in energy exciton resonance, obtained by fitting each measured spectrum using expressions (1) and (2). A good fit is obtained for this dependence using the standard expression [1, 7]

$$\hbar\Gamma_N(T) = \hbar\Gamma_N(0) + \hbar\gamma_{ac}T + \frac{\hbar\gamma_{LO}}{\exp(kT/E_{LO}) - 1}. \quad (3)$$

Here, the first term describes nonradiative broadening at zero temperature, while the second and third terms describe the increase in broadening due to the scattering of excitons by acoustic and optical phonons, respectively.

As can be seen from the figure, the broadening grows linearly with temperature up to $T \approx 60 \text{ K}$ and is thus determined predominantly by scattering on acoustic phonons. Scattering constants $\hbar\gamma_{ac}$ have similar values for all of the investigated exciton states. For example, $\hbar\gamma_{ac} = 0.65 \mu\text{eV/K}$ for resonance X1, while $\hbar\gamma_{ac} = 0.75 \mu\text{eV/K}$ for resonance X4. These values are

slightly less than the $\hbar\gamma_{ac} = 1.1 \mu\text{eV/K}$ obtained in [1] for narrow QWs.

A rapid rise in nonradiative broadening is observed at higher temperatures. This is explained by exciton scattering on thermally-activated optical phonons (mainly longitudinal optical (LO) phonons) [7]. It is described well by the last term in expression (3). Fitting yields values of $\hbar\gamma_{LO} = 5.3 \text{ meV}$ and $E_{LO} = 29 \text{ meV}$ for resonance X1, along with $\hbar\gamma_{LO} = 13 \text{ meV}$ and $E_{LO} = 33 \text{ meV}$ for resonance X4. These data agree with those in [1]. The values obtained for the LO-phonon energy are slightly lower than the one for crystal GaAs: $E_{LO} = 37 \text{ meV}$ [8].

EXCITON–EXCITON AND EXCITON–CARRIER SCATTERING

Optical excitation above the lowest exciton transition can be followed by the creation of excitons with large wave vectors in the QW plane that exceed the wave vector of light in the QW layer. Such excitons do not interact with light and can exist for several tens of nanoseconds in high-quality heterostructures [2]. As a result, a reservoir of nonradiative excitons is created with an areal density of excitons by orders of magnitude exceeding those of radiative excitons. Even at weak optical excitation, the accumulation of nonradiative excitons is possible, which could result in strong broadening of the exciton lines due to exciton–exciton collisions.

Additional monochromatic excitation of the sample was used to study the scattering of radiative and nonradiative excitons. The photon energy of the excitation was varied continuously; for each photon energy, the reflectance spectrum was measured and the degree of inhomogeneous broadening was determined. As a result, the spectral dependence of the inhomogeneous broadening was found. In analogy to the photoluminescence excitation spectrum, this dependence can be referred to as the excitation spectrum of inhomogeneous broadening.

The example of the spectrum for resonance X1 can be seen in Fig. 3, where a number of maxima marked as X1, ..., X10 and Xlh are observed. The spectral positions of these maxima coincide with those of exciton resonances in the reflectance spectra. They may therefore be considered a result of the resonant excitation of excitons, followed by their escape from the light cone due to a variety of scattering processes. The nonradiative excitons created in this manner are efficiently accumulated in the reservoir. The population of the reservoir via such processes is clear from the resonant increase in the constant of nonradiative broadening. A similar effect is observed upon the excitation of light-hole excitons. This feature is marked in Fig. 3 by Xlh.

A continuous excitation spectrum of exciton scattering is observed in addition to the resonant features.

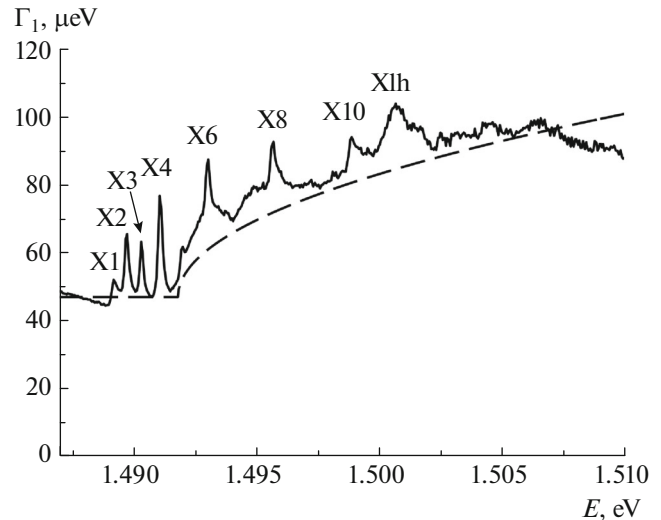


Fig. 3. Excitation spectrum of the nonradiative broadening of exciton resonance X1 (solid curve). The dashed curve is the spectral dependence of the carrier density of states described by expression (4).

It takes the form of a pedestal at around $50 \mu\text{eV}$ and has the smoothly growing background shown in Fig. 3 by the dashed line. This background is well approximated by the square-root dependence

$$\Gamma_N = A_c \sqrt{E - E_g}, \quad (4)$$

where E_g is the bandgap in the QW and A_c is the fitting parameter. The observed effect of the smoothly growing intensity of exciton scattering can be attributed to the photocreation of uncoupled (free) electrons and holes. The density of states of free carriers (and thus the light absorption coefficient in direct-gap semiconductors) is described by a square-root dependence on the photon energy similar to expression (4) [8]. The increase in the carrier concentration is correspondingly described by a similar dependence when the optical excitation power is conserved. The efficiency of exciton scattering by free carriers is considerably higher than that of scattering by nonradiative excitons [9, 10], so even relatively low absorption relative to resonant absorption produces an easily observable effect. It is worth noting that in QWs, the absorption spectrum resulting from the creation of free carriers has a step-like profile [11]. With the investigated QW, however, in which there are many quantum-confined exciton states, the distance between the energies of the states is small, and the square-root function is a good approximation. Our experiment shows that the amplitudes of the resonant features, the pedestal, and the growing background are very sensitive to sample temperature and the power of optical excitation. This opens up possibilities for quantitative study of the cross sections of exciton–exciton and exciton–free carrier scatterings under different experimental condi-

tions. Investigating these effects is a topic for a separate work.

CONCLUSIONS

Reflectance spectroscopy in combination with additional optical excitation allows us to investigate different processes of exciton scattering in semiconductor heterostructures. Measurements of the reflectance at different sample temperatures allows us to study the scattering of excitons by phonons and determine the parameters of scattering. The parameters of scattering for the acoustic phonons obtained in this work have the lowest values of those reported in the literature so far. Excitation spectroscopy of the nonradiative broadening allows us to study the spectral dependences of exciton–exciton and exciton–free carrier scatterings. In the excitation spectra of nonradiative broadening, exciton–exciton scattering produces narrow resonances at the energies of the quantum-confined exciton states. Scattering by free carriers produces a smoothly varying background in the spectrum of nonradiative broadening. Quantitative study of the parameters of exciton–exciton and exciton–free carrier scattering requires further development of experimental means that would allow determination of the concentration of excitons in a reservoir and the concentration of free carriers.

The study of nonradiative broadening by means of reflectance spectroscopy is possible only for high-quality heterostructures in which the inhomogeneous broadening of exciton lines is considerably less than the homogeneous broadening. Analysis of the reflectance spectra is complicated when the broadenings are comparable. Statistics of the spread of the exciton transition energies must be considered in expressions (1) and (2). Analysis shows that the reliability of the results obtained in this manner rapidly drops upon an increase in inhomogeneous broadening.

ACKNOWLEDGMENTS

The authors thank P.S. Grigoryev and I.Ya. Gerlovin for their helpful comments on this work. They are also grateful to the Nanophotonics resource center of St. Petersburg State University (www.photon.spbu.ru) for providing the sample studied in this work.

This work was supported by the Ministry of Education and Science of the Russian Federation on the framework of the Russian–Greece project no. RFMEFI61617X0085.

REFERENCES

1. Poltavtsev, S.V., Efimov, Yu.P., Dolgikh, Yu.K., et al., *Solid State Commun.*, 2014, vol. 199, p. 47.
2. Trifonov, A.V., Korotan, S.N., Kurdyubov, A.S., et al., *Phys. Rev. B*, 2015, vol. 91, p. 115307.
3. Grigoryev, P.S., Kurdyubov, A.S., Kuznetsova, M.S., et al., *Superlattices Microstruct.*, 2016, vol. 97, p. 452.
4. Ivchenko, E.L., *Optical Spectroscopy of Semiconductor Nanostructures*, Springer, 2004.
5. Grigoryev, P.S., Exciton spectroscopy in heterostructures with quantum wells in a magnetic field, *Cand. Sci. (Phys.–Math.) Dissertation*, St. Petersburg: St. Petersburg State Univ., 2016.
6. Shah, J., *Ultrafast Spectroscopy of Semiconductors and Semiconductor Nanostructures*, Springer, 1996.
7. Lee, J., Koteles, E.S., and Vassell, M.O., *Phys. Rev. B*, 1986, vol. 33, p. 5512.
8. Yu, P.Y. and Cardona, M., *Fundamentals of Semiconductors: Physics and Materials Properties*, Springer, 1999.
9. Honold, A., Schultheis, L., Kuhl, J., and Tu, C.W., *Phys. Rev. B*, 1989, vol. 40, p. 6442.
10. Bajoni, D., Senellart, P., Perrin, M., et al., *Phys. Status Solidi B*, 2006, vol. 243, p. 2384.
11. Davies, J.H., *The Physics of Low-dimensional Semiconductors: An Introduction*, Cambridge Univ. Press, 1998.